Genes & Diseases (2023) 10, 2263–2266

Available online at www.sciencedirect.com

ScienceDirect

journal homepage: www.keaipublishing.com/en/journals/genes-diseases

RAPID COMMUNICATION

# A novel variant of GALC in a familial case of Krabbe disease: Insights from structural bioinformatics and molecular dynamics simulation

Krabbe disease or globoid cell leukodystrophy (GLD; MIM# 245200) is a rare and fatal lysosomal storage disease with an autosomal recessive mode of inheritance that results from the deficiency of galactocerebrosidase (GALC; E.C. 3.2.1.46), a lysosomal enzyme encoded by the GALC gene.[1] GALC breaks down galactosylceramide, a cerebroside located mainly in the myelin sheath. Defects in GALC cause the accumulation of a cytotoxic metabolite, galactosylsphingosine or psychosine, which can be toxic to oligodendrocytes and Schwann cells.[2] The failure to digest galactosylceramide triggers the formation of multi-nucleated globoid cells, causing severe demyelination, axonopathy, and neuronal death.[3] The reported frequency of Krabbe disease is 1 in 100,000 live births with symptoms including irritability, loss of motor ability, spasticity, ataxia, visual dysfunction, seizures, and cognitive impairment.[4]

The GALC gene is located on chromosome 14q31 and contains 17 exons spanning 60 kb.[5] In this study, 10 members of a consanguineous family from Swat district, Khyber Pakhtunkhwa, Pakistan were analyzed. Three affected individuals in two generations that includes two males aged 25 and 10 (IV-4 and V-1) and a female aged 23 (IV-5) were diagnosed with Krabbe disease. Patients IV-4 and V-1 were bedridden with several symptoms (poor coordination, progressive loss of vision, spasticity, progressive weakness, and loss of muscle mass). Patient IV-5 was not bedridden; however, her symptoms were the same as those of the other two male patients. The pedigree of the selected consanguineous family (Fig. 1A), magnetic resonance imaging scans, and data of the patients and their symptoms are shown in the supporting information (Fig. S1–3 and Table S1).

The causative gene in the family was investigated through whole exome sequencing of the affected individuals (Patients IV-4 and IV-5). The proband was diagnosed with Krabbe disease with a novel homozygous variant (NM_000153.3; c.449C > T; p. Pro150Leu) in GALC. A total of 105,375 and 102,893 variants were identified in proband IV-4 and IV-5, respectively, and 21 pathogenic variants were retrieved in the preliminary investigation. According to the SIFT, MutationTaster, PolyPhen, and PROVEAN scores, this variant (c.449 C > T; p. Pro150Leu) in *GALC* is the possible cause of this phenotype in the family being studied. After functional annotation, the homozygous variant (c.449 C > T; p. Pro150Leu) in *GALC* was selected for further studies. This gene was sequenced from the rest of the family members by Sanger sequencing (Fig. S4), which showed that the proband's parents (III-1 and III-2) along with other unaffected members (IV-3, IV-6, V-2, and V-4) are heterozygous carriers of the *GALC* variant, and IV-8 is a wild type (WT). This *GALC* variant (c.449 C > T; p. Pro150Leu) was not found in public databases (gnomAD, 1000 Genomes Browser, and HGMD); thus, it is a novel mutation and is likely to be pathogenic.

The structures of WT and mutated (P150L) human galactosylceramidase were predicted *in silico*. Human GALC is composed of 644 residues, arranged in the TIM-barrel (residues 41–337), β-sandwich domain (338–452), and lectin domain (472–668). In the active site, Thr109, Trp151, Asn197, and Arg396 are involved in substrate binding, while Glu198 and Glu274 as catalytic residues serve as proton donor/acceptor and nucleophile for the substrate, respectively. The predicted binding mode of the substrate (β-D-galactocerebroside) in both proteins

Peer review under responsibility of Chongqing Medical University.

https://doi.org/10.1016/j.gendis.2023.01.018

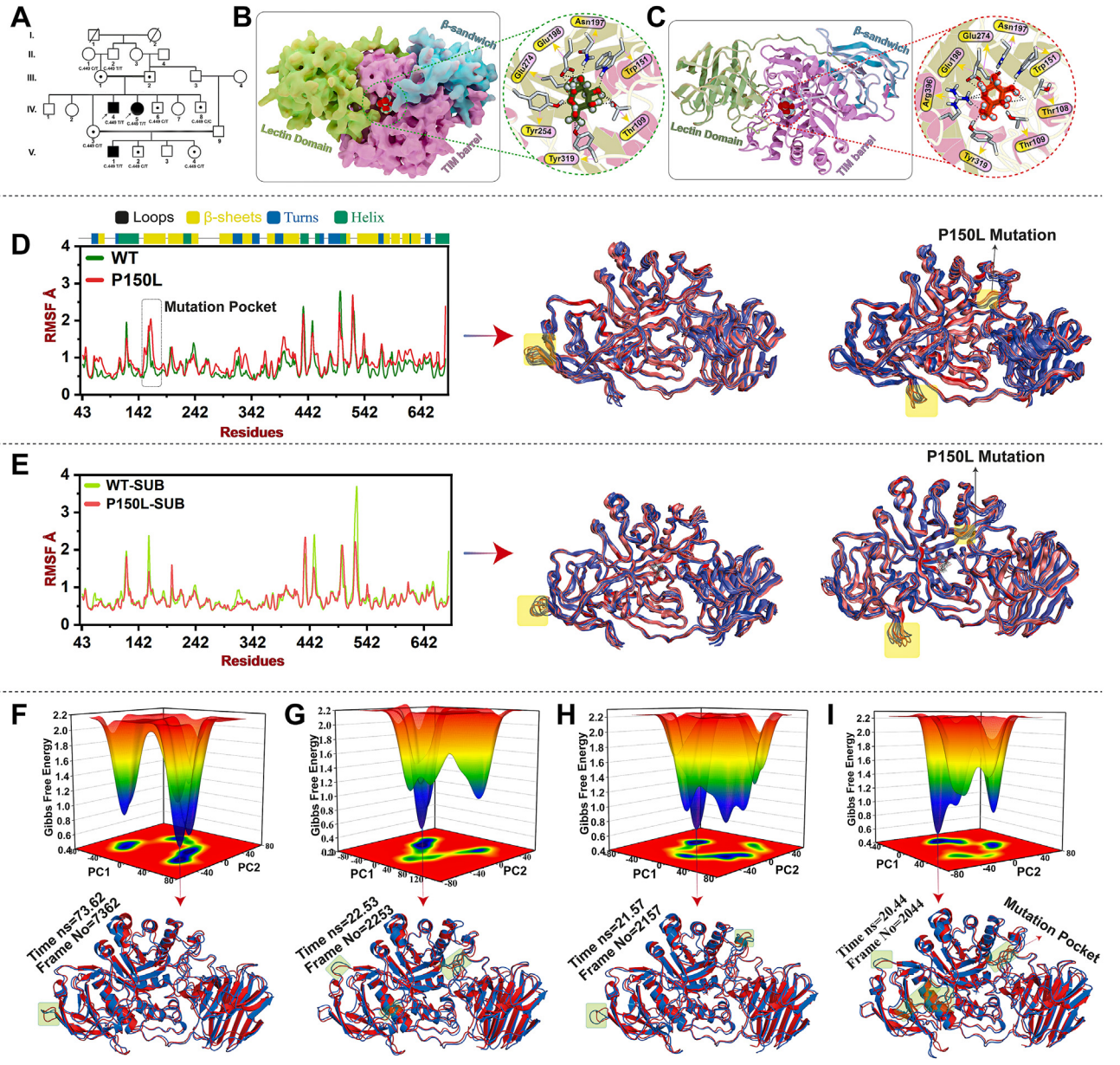


**Figure 1** The presentation of the overall work scheme carried out in this study. **(A)** The pedigree of the consanguineous family with Krabbe disease shows an autosomal recessive mode of inheritance. Whole exome sequencing of two patients was performed, and the probands are indicated by an arrow. **(B)** The 3D structure of human GALC is depicted in the surface and cartoon models. The interactions of substrates are shown in the active site of **(B)** WT and **(C)** P150L. The interacting residues are depicted in the red stick model, hydrogen bonds are shown in red dotted lines, and the ligand is presented with a green ball and a stick model. **(D)** Root mean square fluctuation analysis of WT and P150L. **(E)** Root mean square fluctuation analysis of WT-SUB and P150L-SUB. Cartoon representation of 10 ensembles taken after every 10 ns of the trajectories of WT, P150L, WT-SUB, and P150L-SUB. The fluctuated loops and mutation pockets are highlighted in yellow. **(F—I)** Free energy landscape of WT, WT-SUB, P150L, and P150L-SUB. The high energy, minimal energy, and intermediate energy states are shown in red, blue, and yellow, respectively. The metastable (blue) and high energy state (red) of each system is shown in a cartoon model. The frame number at which the system acquires a metastable state with the time (ns) is reported in Table S5 for each system.

revealed substrate hydrogen bonding (H-bonding) with Gly64, Thr109, Trp151, Asn197, Glu198, Tyr254, and Glu274, and hydrophobic interactions with Trp307 in the active site of WT [docking score (DS) = −5.171 kcal/mol]. In P150L, substrates exhibit higher DS (−5.440 kcal/mol) due to additional H-bonding with Thr108, Tyr319, and Arg396 along with Gly64, Thr109, Trp151, Asn197, Glu198, and Glu274 (Table S2—4 and Fig. S5—8; Fig. 1B, C).

The effects of P150L mutation on the structure and dynamics of GALC were investigated through molecular dynamic simulation (of 100 ns) using the coordinates of WT, P150L, WT-SUB (a complex of WT and a substrate), and

P150L-SUB (a complex of P150L and a substrate). The root-mean-square deviation (RMSD), RMSD distribution plot, and radius of gyration (Fig. S9) indicate that P150L mutation destabilizes the protein, and consequently affects the activation and de-activation of the protein. Root mean square fluctuation (RMSF; Fig. 1D, E; Fig. S10) revealed that substrate binding induces favorable conformational changes in WT-SUB, which is restricted in P150L-SUB; thus, mutation forbids P150L to undergo the structural/conformational rearrangement required for the proper functioning of the protein. The functional motion in the protein was studied through principal component analysis and porcupine plot (Fig. S11—13) that showed highly significant motion (52%) in P150L due to rearrangement of residues upon mutation with 41%, 29%, and 39% variance of motion in WT, P150L-SUB, and WT-SUB, respectively. Upon ligand binding, WT-SUB acquired high energy conformation to gain functional activation motion, and P150L-SUB motion was reduced to prevent the protein from conformational shifts. The active site was opened in WT due to the rotation of the lectin and β-sandwich domains, whereas it was closed in the WT-SUB. In P150L, the lectin and β-sandwich domains were moved in an inward direction, disturbing the active site by partial closure, whereas these domains moved away from the active site in P150L-SUB, partially opened the active site, and disrupted the protein conformation (Videos S1—4). Consequently, mutation near the active site significantly affected the compactness of protein and altered the biological activity of the enzyme.

Free energy landscape (FEL; Fig. 1F—I and Table S5) and dynamic cross-correlation map (DCCM) were used to understand the mechanism of transition and to describe the overall residual correlated motion in WT/P150L/WT-SUB/P150L-SUB. In FEL, P150L/P150L-SUB acquired a high energy state compared with WT/WT-SUB. The total energy of P150L-SUB (−9200 to −9600 kcal/mol) was higher than that of P150L (−9400 kcal/mol), WT (−9200 to −9400 kcal/mol), and WT-SUB (−9300 to −9500 kcal/mol), indicating its instability and structural variation. In DCCM, the difference in the correlation motion between WT and P150L was dominant in the ϒ3 region (mutation pocket) of P150L. The β2/β5/T7 and β11/β12 of P150L showed strong positive and strong negative correlation motions, respectively, compared with WT; these motions are absent in WT-SUB. P150L-SUB showed only moderate positive correlation motion in H1/ϒ3; therefore, mutation restricts the residual movement (Fig. S14—16). This is also confirmed by different H-bonds analyses in WT/P150L/WT-SUB/P150L-SUB, which proves that structural variation in P150L-SUB inhibits the functional motion of protein upon ligand binding. In the active site of P150L, the substrate mediates more interactions compared with WT due to the mutation near the active site, which leads to an increase in the substrate's interaction energy and alters the function of GALC (Fig. S17, 18). Furthermore, SASA analysis revealed an increase in the surface area of P150L (>24,000 Å$^2$) compared with that of WT (∼23,000 Å$^2$), whereas substrate binding decreased the surface area of P150L-SUB (∼22,000 Å$^2$) compared with that of WT-SUB (23,000 Å$^2$). The increased SASA of WT-SUB validates that mutation disrupts the functional motion of P150L (Fig. S19).

In MM-GBSA, a difference in energy was noted between WT-SUB and P150L-SUB. P150L-SUB exhibited higher $\Delta_{VDW}$, $\Delta_{EEL}$, and $\Delta_{G\ TOTAL}$ than $\Delta_{VDW}$, $\Delta_{EEL}$, and $\Delta_{G\ TOTAL}$ of WT-SUB with varied complex—receptor—ligand (C-R-L) difference of WT-SUB (−32.27) and P150L-SUB (−35.73). $\Delta_{EGB}$ and $\Delta_{SASA}$ of P150L-SUB were less than $\Delta_{EGB}$ and $\Delta_{SASA}$ of WT-SUB due to the binding of the substrate with extra residues in the active site of P150L-SUB. MM-PBSA also supported our MM-GBSA results, where $\Delta_{VDW}$ and $\Delta_{EEL}$ of P150L-SUB were increased and $\Delta_{EPB}$ and $\Delta_{SASA}$ were less than the $\Delta_{EPB}$ and $\Delta_{SASA}$ of WT-SUB, with a slightly lower $\Delta_{G\ TOTAL}$ in P150L-SUB (−57920.09) compared with that of WT-SUB (−57955.96). The C-R-L difference was higher in P150L-SUB (Table S6). These results signify that conformational variation in the mutant GALC destabilizes the structure of protein upon mutation, thus supporting deleterious effects on the gene product; therefore, this novel mutation can be classified as a pathogenic variant.

## Conflict of interests

The authors declare that there are no competing interests.

## Funding

This work was funded by the Higher Education Comission of Pakistan (No. NRPU-20—17341).

## Appendix A. Supplementary data

Supplementary data to this article can be found online at https://doi.org/10.1016/j.gendis.2023.01.018.

## References

1. Bradbury AM, Bongarzone ER, Sands MS. Krabbe disease: new hope for an old disease. *Neurosci Lett*. 2021;752:135841.
2. Li Y, Miller CA, Shea LK, et al. Enhanced efficacy and increased long-term toxicity of CNS-directed, AAV-based combination therapy for Krabbe disease. *Mol Ther*. 2021;29(2):691—701.
3. Papini N, Giallanza C, Brioschi L, et al. Galactocerebrosidase deficiency induces an increase in lactosylceramide content: a new hallmark of Krabbe disease? *Int J Biochem Cell Biol*. 2022;145:106184.
4. Wenger DA, Luzi P, Rafi MA. Advances in the diagnosis and treatment of Krabbe disease. *Int J Neonatal Screen*. 2021;7(3):57.
5. Graziano ACE, Cardile V. History, genetic, and recent advances on Krabbe disease. *Gene*. 2015;555(1):2—13.

Ikram Ullah [a,1], Muhammad Waqas [b,c,1], Muhammad Ilyas [a,d,e,**], Sobia Ahsan Halim [c,1], Akmal Ahmad [b], Natalia Dominik [e], Wahid Ullah [a], Muhammad Abbas [a], Muhammad Aamir [a], SYNaPS Study

Group[e], Queen Square Genomics[e], Henry Houlden [e], Stephanie Efthymiou [e], Ajmal Khan [c,*], Ahmed Al-Harrasi [c,***]

[a] *Centre for Omic Sciences, Islamia College University Peshawar, Peshawar, Khyber Pakhtunkhwa 25120, Pakistan*
[b] *Department of Biotechnology and Genetic Engineering, Hazara University, Mansehra, Dhodial 21120, Pakistan*
[c] *Natural and Medical Sciences Research Center, University of Nizwa, Nizwa 616, Sultanate of Oman*
[d] *Department of Bioengineering, University of Engineering and Applied Sciences, Swat, Khyber Pakhtunkhwa 19060, Pakistan*
[e] *Department of Neuromuscular Disorders, UCL Queen Square Institute of Neurology, London WC1N 3BG, United Kingdom*

*Corresponding author.

**Corresponding author. Centre for Omic Sciences, Islamia College University Peshawar, Peshawar, Khyber Pakhtunkhwa 25120, Pakistan.

***Corresponding author.
*E-mail addresses:* milyaskh@hotmail.com (M. Ilyas), ajmalkhan@unizwa.edu.om (A. Khan), aharrasi@unizwa.edu.om (A. Al-Harrasi)

10 May 2022
Available online 23 April 2023

[1] These authors contributed equally to the work.